

# A Drift-Diffusion Model of Pinned Photodiode Enabling Opto-Electronic Circuit Simulation

Yanmei Su, Laidong Wang, Xinnan Lin, and Jin he  
 The key Laboratory of Integrated Microsystems  
 School of Computer & Information Engineering, Peking  
 University Shenzhen Graduate School  
 Shenzhen 518055, P.R.China  
[xinlin@pkusz.edu.cn](mailto:xinlin@pkusz.edu.cn)

Yanmei Su, Xiaojin Zhao, Yu Cao, Dongwei Zhang,  
 Yongliang Li, and Jin He  
 Peking University Shenzhen SOC Key Laboratory  
 PKU-HKUST Shenzhen-Hongkong Institute  
 Shenzhen 518057, P.R.China  
 Tel: 86-755-260324 Fax: 86-755-26033249  
[hejin@szpku.edu.cn](mailto:hejin@szpku.edu.cn)

**Abstract**—A drift-diffusion analytical model with bounded boundary conditions for CMOS image sensors (CIS) in a vertical pinned photodiode (PPD) is presented in this paper. According to the comparison with the numerical simulation and measured data, this model has been proved to be valid for fast simulation of optoelectronic integrated circuit (OEIC). Furthermore, it has been implemented into Hspice, to capture the specific characteristics of sensor applications with PPDs. This PPD model including concise mathematical formulation of carrier transport mechanism is useful in developing generic compact models which includes the advanced physical effects.

**Keywords**—Drift-Diffusion model, Pinned Photodiode, CMOS Image Sensors

## I. INTRODUCTION

Recently, complementary metal-oxide-semiconductor (CMOS) image sensors (CIS) is widely applied for consumer electronics [1], and lots of research in circuit performances and devices improvement has been devoted by numerical simulation and experiments. However, the process manufacturing and the pixel architecture are found to have a great influence on optical characteristics with the device scaling down. Hence, to overcome the inefficient and high-cost of numerical simulations and experiments, an accurate physics-based analytical compact model of OEICs is in urgent demand. Although the photodiode model, as the core module of OEICs incorporated optical devices into conventional VLSI, has been researched with intense vigor [2]. Yet, the HiSIM-photodiode (HiSIM-PD) model, which is a physics-based model for p-i-n PD under unbound boundary conditions, only proposes a numerical expression with a constant electric field. Besides, the PPD structure originally develops for charge coupled device (CCD) image sensors, to extensively apply for CISs to reduce dark current and transfer noise. Therefore, a precise analytical PPD is extremely important. In our work, based on a general electric field function obtained from Poisson's equation, a drift-diffusion analytic model of PPD with bounded boundary is proposed and implemented in Hspice to investigate the characteristic of a two-stage charge transfer (TSCT) pixel, which structure is reported in [3]. The

comparison among the model, 2-D numerical simulation and measured data is directly performed to confirm the PPD model. Consequently, the physical analytic PPD model, having an open structure, combined with BSIM model, can be adapted to study advanced physical effects under different structural parameters and a wide range of wavelengths of incident illumination in future.

## II. PHOTO CURRENT MODEL OF PPD

### A. The building of photocurrent in PPD

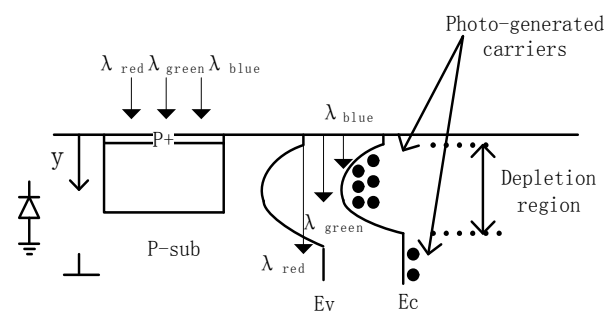


Figure.1 Structure of the Pinned Photodiode is shown here. Incident photons penetrate into the semi-conduction according to their energy or wavelength; photons with smaller energy or longer wavelength penetrate deep into the device, while photons with larger energy or shorter wavelength are absorbed near the surface.

Figure.1 schematically shows the device structure of a PPD. The main subjects of the PPD-model development are the carrier generation process due to photo excitation and the carrier flows across the depletion region. Modeling of the photocurrent response begins with the current continuity equations for electrons and holes described as below:

$$\frac{\partial n_{e,h}(y,t)}{\partial t} - \frac{1}{q} \frac{\partial J_{e,h}(y,t)}{\partial y} = G_{e,h}(y,t) - R_{e,h}(y,t) \quad (1)$$

$$J_{e,h}(y,t) = -D_{e,h} \nabla n_{e,h}(y,t) + \mu_{e,h} n_{e,h}(y,t) E(y) \quad (2)$$

where  $n_e$  and  $n_h$  are the electron and hole concentrations respectively.  $\mu_{e,h}$  is the effective carrier mobility of electron or hole;  $D_{e,h}$  is the diffusion coefficient of electron or hole, which

determined by Einstein relation.  $J_{e,h}(y,t)$  is the current density along the p-n direction (the direction);  $R_{e,h}$  is the recombination rate and  $G_{e,h}$  is the carrier generation rate. The subscript  $n_{e,h}(y,t)$  represents electron and hole along the direction. Since carrier generation in PPDs is mainly caused by the photo excitation, generation rates of electrons and holes in silicon are assumed to be identical under a certain wavelength of incident illumination. The carrier generation rate at the distance from the PPD structure surface is expressed as

$$G_{e,h}(y,t) = \eta_Q \alpha \Phi_{e,h} e \quad (3)$$

where  $\eta_Q$  is the diffraction light energy efficiency described by constant-light-diffraction-scaling (CLDS) methodology;  $\alpha$  is the light attenuation coefficient;  $\Phi_{e,h}$  is optical photon flux. Note that a general electric field function obtains from Poisson's equation, and the mobility and the lifetime expressions of minority carriers combine with various effects. In order to solve Equations (1)-(2), analytically, we divide the physical region into two parts, one is the drift-domain region, and the other is diffusion-domain one. In the drift-domain region, we employ those transformations in drift-domain region as follows:

$$b_A = \frac{E_{p,plus} n_{e,h}}{Y_{n1}} \quad (4)$$

$$c_A = -\frac{E_{p,plus} n_{e,h}}{Y_{n1}} (Y_{n1} + H_{p,plus}) \quad (5)$$

$$c_B = \frac{\mu_{e,h} E_{p,plus} n_{e,h}}{Y_{n1}} + \frac{1}{\tau_{e,h}} \quad (6)$$

$$a_C = \eta_Q \alpha \Phi_{e,h} \quad (7)$$

$$c_C = \frac{n_{e,h,0}}{\tau_{e,h}} \quad (8)$$

where  $\tau_{e,h}$  is the effective lifetime of carriers of electron or hole;  $E_{p,plus}$  is the maximum value of electric field between  $P_{plus}$  region and N region;  $Y_{n1}$  is the width in the N region under equilibrium state;  $H_{p,plus}$  is the height of  $P_{plus}$  region;  $n_{e,h,0}$  is the equilibrium carrier density in N region. The final expression of the density of electron and hole along the direction in drift-domain region,  $n_{e,h}$  is evaluated as

$$n_{e,h}(y) = C_{e1} (c_A + b_A y)^{\frac{c_B}{b_A}} \left\{ \frac{c_C}{c_B} - \frac{1}{b_A} \left( a_C e^{\frac{\alpha c_A y}{b_A}} \right) \left[ \frac{\alpha (c_A + b_A y)}{b_A} \right]^{\frac{c_B}{b_A}} \right\} \quad (9)$$

where  $\Gamma \left[ \frac{c_B}{b_A}, \frac{\alpha (c_A + b_A y)}{b_A} \right]$  is a Gamma Function, which can be described as  $\Gamma(z, a) = \int_a^{\infty} e^{-t} t^{z-1} dt$ , and the accurate parameter expressions of  $C_{(e,h)1}$ ,  $C_{(e,h)2}$  can be calculated by the specific bounded boundary conditions.

In diffusion-domain region, we can get the solution as follow:

$$n_{e,h}(y) = D_{(e,h)1} e^{\frac{y}{L_{e,h}}} + D_{(e,h)2} e^{-\frac{y}{L_{e,h}}} + \frac{\eta_Q \alpha \Phi_{e,h} \tau_{e,h}}{1 - \alpha^2 L_{e,h}^2} e^{-\alpha y} + n_{e,h,p0} \quad (10)$$

where  $L_{e,h}$  is diffusion length, and the parameters  $D_{(e,h)1}$ ,  $D_{(e,h)2}$  can be calculated by the defined boundary.

Combining with the absorption coefficient and absorption length of silicon under different wavelengths of incident light in Figure.2, the carrier distributions in different intensity of incident illumination under different structural parameters are shown in Figure.3, Figure.4, Figure.5, and Figure.6.

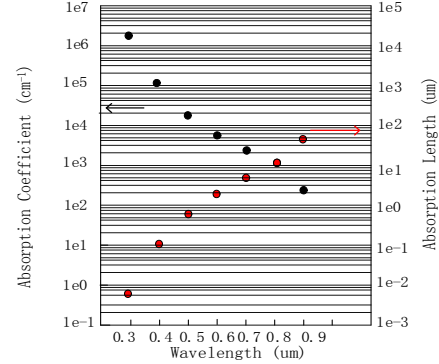


Figure.2 Absorption coefficients (black point) and absorption lengths (red point) of silicon as a function of wavelength are presented here, as presented in [1]

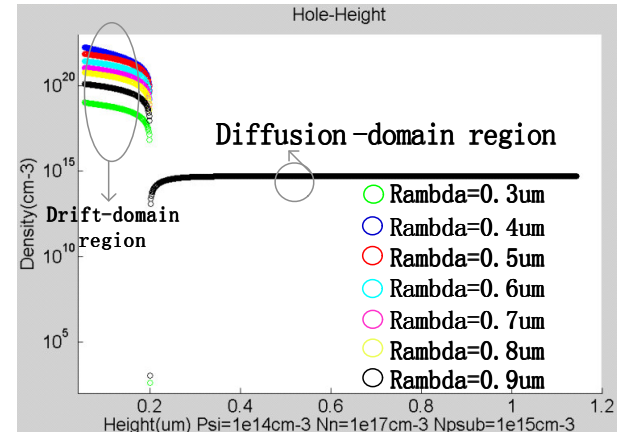


Figure.3 The carrier distribution of hole along y-axis in Pinned Photodiode is presented here when the wavelength of incident light is 0.3um

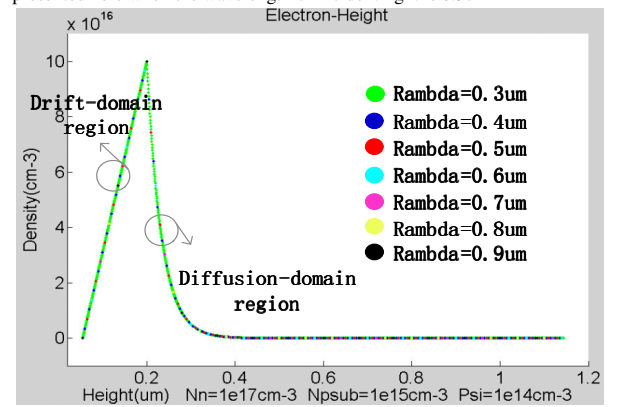


Figure.4 The carrier distribution of electron along y-axis in Pinned Photodiode is presented here when the wavelength of incident light is 0.3um

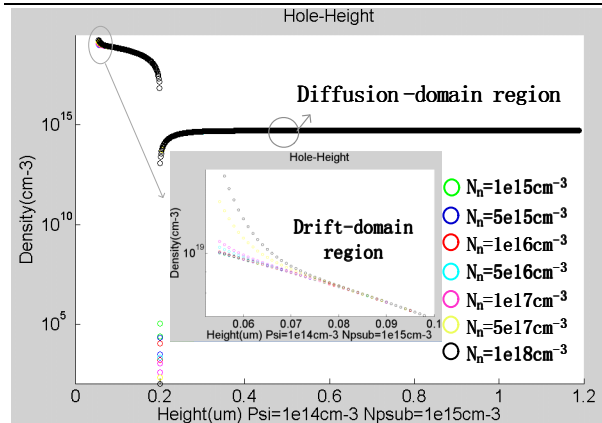


Figure.5 The carrier distribution of hole along  $y$ -axis under different donor doping concentration in the Pinned Photodiode is presented here when the wavelength of incident light is  $0.3\mu\text{m}$ , which shows that the hole in drift-domain region is sensitive with donor doping, while the diffusion-domain region is not.

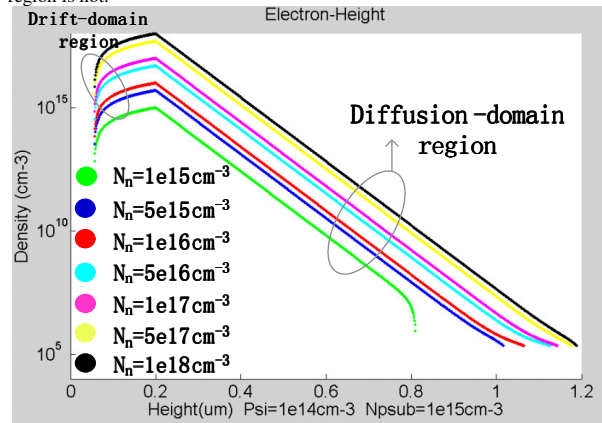


Figure.6 The carrier distribution of electron along  $y$ -axis under different donor doping concentration in the Pinned Photodiode is presented here when the wavelength of incident light is  $0.3\mu\text{m}$ , which reveals that the electron is directly bound up with donor doping concentration in both drift-domain region and diffusion-domain one.

In addition, because of the high potential barrier in the photodiode depletion region, the hole is blocked in the  $P_{\text{plus}}$  region. Hence, the electron becomes the main composition of photocurrent in solar cell mode. Furthermore, combining with the accumulation mode of photodiode, the photocurrent can be calculated by

$$I_{\text{ppd}} = J_e(y_0)A + I_{\text{ph}} \quad (11)$$

where

$$I_{\text{ph}} = P_{\text{opt}} R_{\text{ph}} L_o A \quad (12)$$

And is any node in PPD junction for the continuity of current. In equation (12), the incident light power  $P_{\text{opt}}$  can be defined as  $P_{\text{opt}} = \Phi_{e,h} h\nu$ , and the sensitivity  $R_{\text{ph}}$  is expressed as  $R_{\text{ph}} = \eta_q \frac{e}{h\nu} = \eta_q \frac{\lambda}{1.23}$ , and  $L_o$  is the illumination at the PPD surface, and  $A$  is the area size of the PPD.

## B. Application to Circuit Simulation

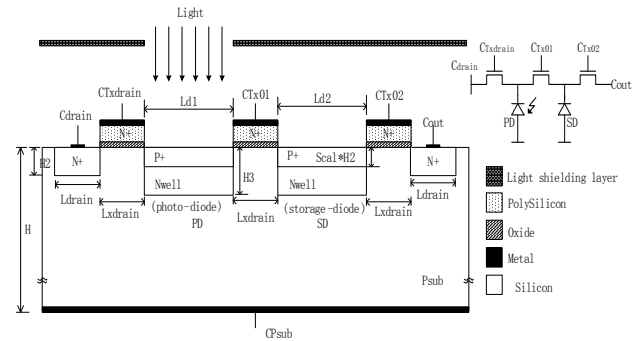


Figure.7 Structure of a CMOS Image Sensor with In-Pixel Two-Stage Charge Transfer, and the structural parameters

The PPD physical model is applied into a two-stage charge transfer (TSCT) pixel [3], which is not only successful used as a new type of global electronic shutter pixel for CISs, but also serves as a fluorescence lifetime imaging that realizes subnanosecond time resolution with two charge transfer stages, as is shown in Figure.7. Moreover, we develop an equivalent circuit of TSCT pixel illustrated in Figure.8 as the [4] operates, to simulate its photo-electrical characteristics in Hspice.

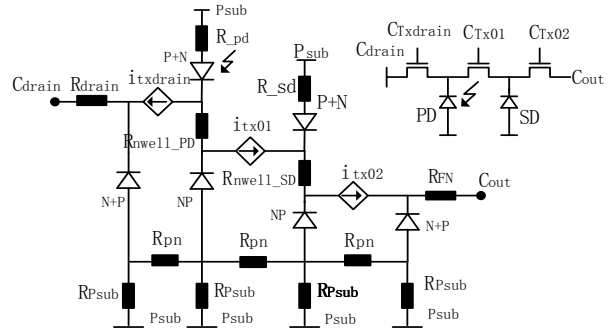


Figure.8 The equivalent circuit of a CMOS Image Sensor with In-Pixel Two-Stage Charge Transfer

Simulation with this PPD model in Hspice, approving the comparison of measured and 2-D numerical simulated data, this PPD model is verified by the Figure.9. As scaling down, the BSIM model of NMOS provides a convenient way to investigate how the advanced physical effects influence on the CIS circuits.

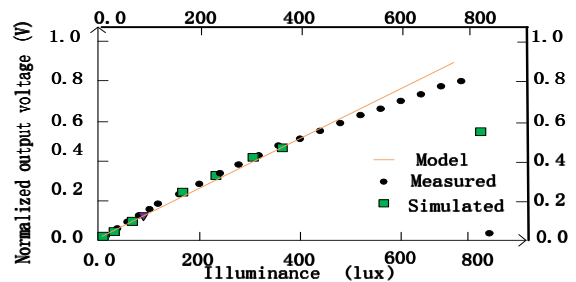


Figure.9 The comparison of Output characteristic among the equivalent circuit model, the measured data and the 2-D simulated data of a CMOS Image Sensor with In-Pixel Two-Stage Charge Transfer

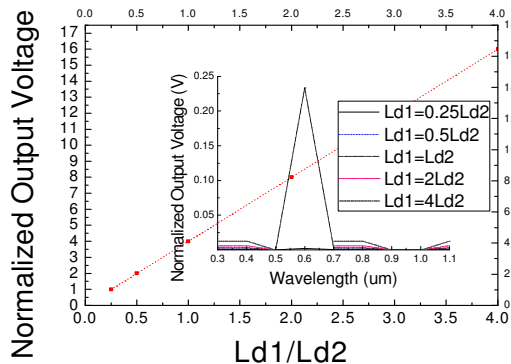


Figure.10 The Output Voltage versus the Length proportion of photodiode compared with storage diode in the model of TSCT pixel, and the response output voltages under different incident wavelengths are also shown.

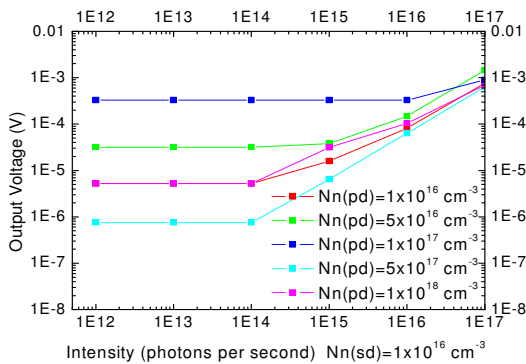


Figure.11 The Output Voltage in photodiode mode versus intensity in different photodiode doping concentration under 0.3um incident light, when  $Ld1=1/3 Ld2$ .

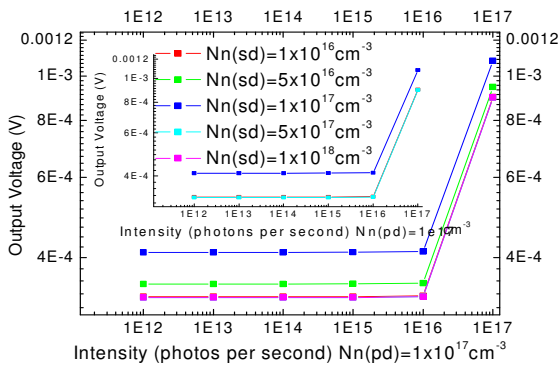


Figure.12 The Output Voltage in photodiode mode versus intensity in different storage-diode doping concentration under 0.3um incident light, when  $Ld1=1/3 Ld2$ .

The Figure.10 demonstrates that the output voltage increases as the  $Ld1/Ld2$  raises, which confirms that the sensitivity of sensor having a direct proportional with photo-absorption area. The Figure.11 shows that the output is a constant under low intensity incident light while the doping level has a great influence on the output characteristic. Additional, the output increases as the photon intensity grows. The output voltage in photodiode mode is about the maximum only when the storage-diode doping density equals to the photodiode doping concentration, and it keeps a constant under low intensity incident light, significantly increases in contrast, as is shown in Figure.12. Therefore, this model successfully predicts not only photodiode performance improvement, but also overall circuit performance.

### III. CONCLUSION

The developed analytical physics-based equations of the PPDs with bounded boundary conditions, includes the velocity saturation effect, accuracy lifetime and mobility expressions under different doping level, which is a powerful tool for optimizing performance of both OEICs simulation. Furthermore, it is applied successful in the TSCT-CIS pixel, which is applicable to estimate the OEICs performance with respect to the improvement of PPD. Therefore, this PPD model sets a stage for the compact model simulation which has been lagging behind numerical efforts so far.

### ACKNOWLEDGMENT

This work is supported by the Key Project of National Natural Science Funds of China (61036004), the Guangdong Natural Science Foundation (10466585979-2004985), This work is also supported by Shenzhen Science & Technology Foundation (CXB201005250031A, JSA200903160146A ), The Fundamental Research Project of Shenzhen Science & Technology Foundation (JC200903160353A, JC201005280670A).

### References

- [1] Jun Ohta, "Smart CMOS Image Sensors and Applications", CRC Press, Taylor & Francis Group, 2008
- [2] T.Ezaki, G.Suzuki, K.Konno, O.Matsushima, Y.Mizukane, D.Navarro, M.Miyake, N.Sadachika, H.J.Mattausch, and M.Miura-Mattausch, "Physics-Based Photodiode Model Enabling Consistent Opto-Electronic Circuit Simulation" International Electron Devices Meeting, December 1-4, 2006
- [3] H.J.Yoon, S.Itoh, and S.Kawahito, "A CMOS Image Sensor With In-Pixel Two-Stage Charge Transfer for Fluorescence Lifetime Imaging", IEEE Trans. ED, Vol.56, No.2, pp.214-221, Feb. 2009
- [4] Yanmei Su, Laidong Wang, Ruonan Wang, Xukai Zhang, Yiqun Wei, Wei Wang, Yong Ma, Xinnan Lin, Jin He, "A Compact Model of Diode Array for Phase Change Memory", EDSSC, pp.1-4, 2010